Colloids and Surfaces A: Physicochem. Eng. Aspects 507 (2016) 134–140

Contents lists available at ScienceDirect

Colloids and Surfaces A: Physicochemical and Engineering Aspects

journal homepage: www.elsevier.com/locate/colsurfa

Important double bond effect on the aggregation behavior of an alkenyl succinic acid derivative

O. Fernando Silva*, Rita H. de Rossi, Mariana A. Fernández

Instituto de Investigaciones en Físico-Química de Córdoba, INFIQC-CONICET, Facultad de Ciencias Químicas, Departamento de Química Orgánica, Universidad Nacional de Córdoba, Ciudad Universitaria, (X5000HUA) Córdoba, Argentina

HIGHLIGHTS

- The aggregation behavior of 2-(2-decenyl) succinic acid in alkaline aqueous media was studied.
- The surfactant have high tendency to self-assembly forming small spherical micelles.
- The double bond in the lateral chain seems to be the responsible of the unusual aggregation behavior.

GRAPHICAL ABSTRACT

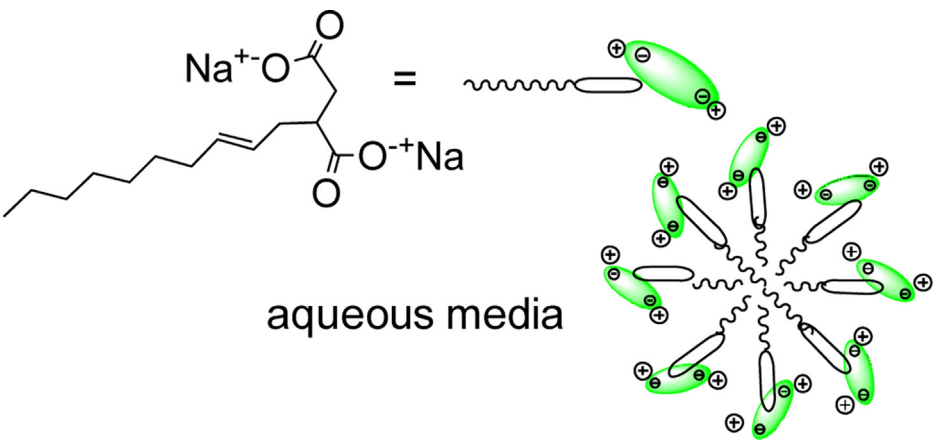

ARTICLE INFO

Article history:
Received 5 July 2016
Received in revised form 26 July 2016
Accepted 31 July 2016
Available online 1 August 2016

Keywords:
Alkenyl succinic acid
Micelles
Aggregation
Langmuir monolayers

ABSTRACT

The aggregation behavior of 2-(2-decenyl) succinic acid (C10SA) in alkaline aqueous media was extensively studied and found interesting properties. The CMC (critical micelle concentration) is lower than expected for a compound with two carboxylate groups and an alkenyl chain of 10–12 carbon atoms. We identified that among the factors that affect the CMC, the double bond and the arrangement of the carbonyl group play a crucial role. They favor an ease packing of the head group of the surfactant resulting in a reduction of their mutual repulsion in the micelle. This particular conformation influences the solubilization/aggregation behavior and is responsible of the high tendency to self-assembly forming micelles of spherical shape and small size. An important feature of C10SA molecules is their ability to orient the carboxyl groups in a way that allow them been packed in the aggregates and this property may be of interest for many future applications.

1. Introduction

Alkenyl succinic anhydrides (ASA) are widely used in different areas, including additives for lubricants, intermediates in organic chemistry, corrosion inhibitors and paper sizing agents [1–3]. In the paper industry, oil-in-water (o/w) emulsions of ASA, are usually employed to impart water resistance to paper and paperboard

* Corresponding author.
E-mail address: fersilva@fcq.unc.edu.ar (O.F. Silva).

http://dx.doi.org/10.1016/j.colsurfa.2016.07.098
0927-7757/

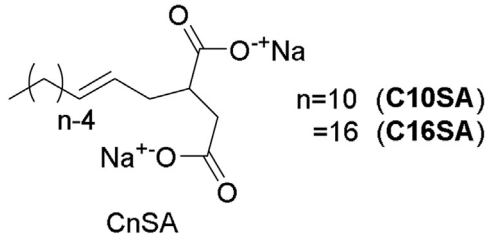

Scheme 1. Structure of surfactants used in this work.

since they confer hydrophobicity to cellulose fibers [3]. However, during the sizing process, ASA are in contact with water and are hydrolyzed to form CnSA (Scheme 1); the calcium or magnesium salts of CnSA cannot be effectively distributed over paper surfaces and form tacky deposits on papermaking equipment. Alternatives to solve this problem leads to the search of new methods to stabilize the emulsions formed with ASA [4–6].

In spite of the technological and economic importance of CnSA in the paper industry and the knowledge that it behaves as a surfactant, there have been, to the best of our knowledge, only a few studies regarding the physicochemical properties of the aggregates of CnSA in water. It has been reported [7,8] that the aqueous solutions of the acid form of C14SA and dipotassium salt of C12SA can form vesicles and small particles with diameters less than 7 μm (in aqueous solutions at pH 5–6). In our laboratory, we observed that C12SA can self-associate (in buffer phosphate at pH = 7) at a very low concentration of surfactant (0.4 mM) [9]. This indicates that C12SA have a highly associative behavior, which is rather surprising in view of the double hydrophilic head and the relatively short tail. On the other hand, research have been performed using CnSA for studies of adhesion interactions [10] and a saturated derivative of C18SA was used in nucleation and control of the inorganic crystal growth in Langmuir experiments [11,12].

Since a key feature of CnSA is their ability to undergo self-assembly in water, a process in which factors such as surfactant molecular structure, surfactant concentration, and temperature dictate the type of aggregates formed; the aim of this work was to describe the aggregation behavior of disodium salt of 2-(2-decenyl) succinic acid C10SA (n = 10, Scheme 1) in alkaline aqueous media. The understanding of the physical chemical mechanism of aggregation and particularly the structural factors responsible for its surfactant efficiency despite its relatively short hydrophobic tail and a big hydrophilic head, will be important for the design of new materials.

2. Experimental section

2.1. Materials

The 2-(2-decenyl) succinic acid and 2-(2-hexadecenyl) succinic acid (C10SA and C16SA in Scheme 1) were obtained from basic hydrolysis of the corresponding alkenyl succinic anhydride prepared as reported previously [2,9]. 0.7 g of alkenyl succinic anhydride (3 mmol) was dissolved with 300 mL of NaOH 0.02 M (6 mmol) and stirred for 12 h. After that time, HCl was added to acidify to pH ≈ 3 producing a white emulsion. The crude product was allowed to cool at 8 °C for 12 h and a white product was collected by filtration. The solid was washed three times with distilled water and afterwards freeze-dried (yield: 90%). Titration of a solution of CnSA prepared in water with NaOH, using phenolphthalein as an indicator, gave a good agreement with the theoretical quantities expected. The structure of the product was confirmed by NMR and FT-IR. NMR spectra show the presence of two rotational isomers (Scheme S1, Supplementary information). The proton (Fig. S1, Supplementary information) and carbon (Fig. S2, Supplementary information) peaks were assigned using 2D COSY and HSQC-DEPT experiments respectively. The existence of rotamers was demonstrated by changing NMR solvents [13,14]. The ^{1}H NMR spectra in $CDCl_3$, and DMSO-d_6 (Fig. S3, Supplementary information) shows the tendency of H_d and $H_{d'}$ signals to coalesce with increasing solvent polarity. In addition, 2D NOESY (^{1}H-^{1}H) experiments showed strong NOE effects (through-space ^{1}H-^{1}H interactions), due the close proximity of the succinic moiety to the double bond region (Fig. S4, Supplementary information).

Acid C10SA: ^{1}H NMR, δ in ppm (400.16 MHz, $CDCl_3$): 0.90 (t, 3H), 1.28 (s, 10H), 2.02 (q, 2H), 2.24 (m, 1H), 2.40–2.60 (m, 2H), 2.56 (m, 1H); 2.89 (broad, 1H), 5.33–5.53 (m, 2H). ^{13}C-NMR, δ in ppm, (100.63 MHz, $CDCl_3$): (mixtures of rotamers) 14.08 (methyl carbon), 22.64; 29.08; 29.12; 29.32; 31.81; 32.46; 34.55; 34.79; 41.24 (methylene carbons and succinic moiety); 124.47; 125.04; 133.81; 134.93 (double bond carbons); 178.59; 180.82 (carboxylic acid groups). FT-IR (KBr, ν_{max}/cm^{-1}): 1687(strong, C=O carboxylic acid), 965 (strong, C=C disubstituted *trans*).

Acid C16SA: ^{1}H NMR, δ in ppm (400.16 MHz, $CDCl_3$): 0.88 (t, 3H), 1.25 (s, 22H), 1.98 (q, 2H), 2.22 (m, 1H), 2.41–2.55 (m, 2H), 2.66 (m, 1H); 2.88 (broad, 1H), 5.27–5.55 (m, 2H). ^{13}C-NMR, δ in ppm, (100.63 MHz, $CDCl_3$): (mixtures of rotamers) 14.11 (methyl carbon), 22.69; 29.16; 29.36; 29.49; 29.62, 29.67, 29.69, 31.93; 41.26 (methylene carbons and succinic moiety); 124.43; 125.01; 134.45; 134.97 (double bond carbons); 178.71; 180.95 (carboxylic acid groups).

FT-IR (KBr, ν_{max}/cm^{-1}): 1692 (strong, C=O carboxylic acid), 968 (strong, C=C disubstituted *trans*).

Saturated acid C10SA was obtained by reduction of the corresponding alkenyl succinic anhydride with catalytic hydrogenation with Pd/C as catalyst in dioxane (P_{H2} = 40 psi, 8 h). The suspension was filtered, dried under reduced pressure and the white solid product was recrystallized twice from boiling water. Yield: 40% ^{1}H NMR, δ in ppm, (400.16 MHz, $CDCl_3$): 0.92 (t, 3H), 1.30 (s, 16H), 1.48–1.55 (broad, 2H), 2.35 (d, 1H), 2.49–2.54 (m, 1H), 2.64 (broad, 1H). ^{13}C-NMR, δ in ppm, (100.63 MHz, $CDCl_3$): (mixtures of rotamers) 14.40 (methyl carbon), 22.54; 26.81; 29.14; 29.29; 29.33, 29.41, 29.42, 31.74; 31.78; 36.13; 41.14 (methylene carbons and succinic moiety); 173.60; 176.45 (carboxylic acid groups). FT-IR (KBr, ν_{max}/cm^{-1}): 1693(strong, C=O carboxylic acid).

2.2. Instruments

A Jasco FP 777 and a Shimadzu Multispect 1501 apparatus were used for spectrofluorimetric and spectrophotometric analyses repectively. Diffusion-Ordered NMR Spectroscopy (DOSY) experiments were carried out on a Bruker Avance II 400 NMR instrument. Surface tensions were measured by the ring method using a Du Noüy ring tensiometer (Cole Parmer Surface Tensiomat 21). Dynamic light scattering measurements were made using Beckman-Coulter Delsa (nanosizer DELSA NANOC).

2.3. General procedures

Unless otherwise mentioned, the aqueous solutions were prepared using buffer $Na_2CO_3/NaHCO_3$, ionic strength of 0.2 M and pH 10.6 using ultrapure water obtained from a Millipore apparatus. An external bath at (25.0 ± 0.1) °C was used for the temperature control of the sample compartment.

In experiments using molecular probes, the procedure was as follows: a stock solution of the probe was prepared in $Na_2CO_3/NaHCO_3$ buffer and the acid form of C10SA was dissolved with an aliquot of this solution, the combination of adequate

volumes of the two stock solutions provided the desired concentrations of all the components

2.4. Critical micelle concentration (CMC) determined by solubilization of Sudan Black

The CMC measurement by solubilization of Sudan Black was performed by adding a low amount of solid dye to solutions of various concentrations of C10SA in buffer. The experiments were done with excess of Sudan Black in each sample (the dye was not completely solubilized), the solutions were placed in a shaker for 24 h and allowed to equilibrate.

2.5. Surface tension measurements

The surface tension (ST) of the solutions was measured and the readings were taken in triplicate to check for the reproducibility, and the averaged values were used for the graphs.

2.6. Dynamic light scattering (DLS)

The apparent hydrodynamic diameters of the micelles were determined at a fixed surfactant concentration of 5 mM tenfold above the CMC. The samples were filtered, prior to use, three times with 0.45 μm PTFE membrane to remove dust or particles. At the scattering angle of 165°, multiple samples and thirty independent size measurements were made for each sample, the polydispersity index of the experiments was always below 0.2. The apparent hydrodynamic diameter values reported using the CONTIN algorithm were weighted by intensity, volume and/or number and no differences were observed between them. DLS experiments show that the standard deviation of the data, using different samples, was less than 10% and the resolution was 0.6 nm.

2.7. Diffusion-ordered NMR spectroscopy (DOSY)

DOSY experiment was performed using a sample of [C10SA] = 5mM in D_2O and adjusting pD∼ 11 with NaOD. The diffusion coefficient was calculated using Topspin 2.1 software. The hydrodynamic radius (R_H) was determined by the Stokes Einstein equation [15].

2.8. Monolayers experiments

Langmuir monolayers were obtained at room temperature by spreading 25 μL of a stock solution of the succinic acid on the surface (80 cm^2) of a 145 mM NaOH sub-phase (78 mL), after five minutes the compression started, and the isotherms did not change between 3 and 15 min. A platinized-Pt sensing plate connected to a surface pressure transducer was used to measure the surface pressure. A high impedance millivolt meter connected to a surface ionizing Am electrode positioned 5 mm above the monolayer surface and to a miniature Ag/AgCl reference electrode submerged in the aqueous sub-phase was used to measure surface (dipole) potential. All the surface pressure-molecular area isotherms reported in this work correspond to those calculated with the measured amount of amphiphile actually present at the interface. The latter was determined by ^{1}H-NMR using benzoic acid as the internal standard and taking the difference between the total amount used and the quantity directly measured in the sub-phase.

Monolayer compressibilities were obtained as reported previously [16].

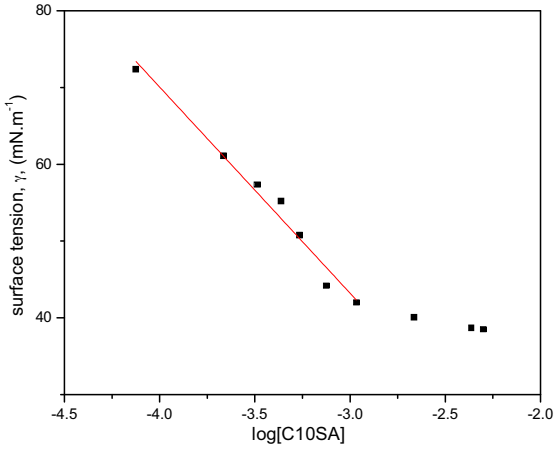

Fig. 1. Surface tension versus log [C10SA]. The cross point is at 1 mM. pH = 10.6, buffer Na_2CO_3/$NaHCO_3$.

Table 1
Values of different micellar parameters determined for C10SA.

CMC (mM)	γ_{cmc} (mN/m)	$10^6.\Gamma_{max}$ (mol/m^2)	A_{min} (nm^2)	R_H (nm)
1.1 [a]	41.8 [a]	4.71[d]	0.35 [d,e]	0.4[f]
0.4[b,c]				0.9 [g]

CMC: critical micelle concentration. γ_{cmc}: surface tension corresponding to CMC. Γ_{max}: maximum surface excess. A_{min}: surface area at the air water interface. R_H: hydrodynamic radius. Measured by: (a) surface tension, (b) fluorescence using tryptamine, (c) UV–vis absorption using Sudan Black, (d) Gibbs adsorption equations, (e) Langmuir monolayers, (f) DOSY and (g) DLS experiments.

3. Results and discussion

3.1. Critical micelle concentration (CMC)

3.1.1. Surface tension method

Fig. 1 shows the plot of surface tension versus log [C10SA]. The CMC value and the surface tension corresponding to CMC (γ_{cmc}) are determined from the breakpoint of the plot (Table 1). After the breakpoint, there is a small decrease in γ upon the C10SA addition and this behavior was also observed for other surfactants, but no conclusive explanation can be offered [17,18].

3.1.2. Fluorimetric and absorption method

The fluorescence spectrum of a solution of tryptamine in buffer did not change upon adding C10SA up to a certain value; then it began to decrease (Fig. S5, Supplementary information). The corresponding value of the abrupt change in slope was assigned to the CMC = 0.4 mM (Table 1).

It should be noted that the aggregates of C10SA quenched the fluorescence of the probe and a similar result was observed previously with other surfactant derived from C10SA [2]. This result was explained considering that the carboxylate group of C10SA can form hydrogen bonds with the amino group of tryptamine.

The determination of CMC by solubilization of Sudan Black leads to a CMC value (Table 1) similar to that of the methods mentioned above. No changes in the absorption intensity at 625 nm were observed up to CMC for C10SA (Fig. S6 in the Supplementary information) and the increase in the absorption intensity at 625 nm occurred at 0.4 mM (CMC), indicating an increase in the amount of the solubilized dye and the appearance/presence of micellar assemblies.

It should be noted that the differences in CMC values obtained from different techniques are usual, which generated the concept

of CMC as a "small region" instead of a single point [17]. Since the CMC values reported in Table 1 are similar between them, a mean value, $CMC_{average} = 0.6 \times 10^{-3}$ M can be calculated.

The CMC values can be compared with those known for sodium alkanoates, such as sodium decanoate [19], tetradecanoate [20] and hexadecanoate [20] which are 50, 1.5 and 0.55 mM respectively. These results are quite striking because the hydrocarbon chain of C10SA is relatively short and the carboxylate groups are expected to form a large hydrophilic head group, both factors are expected to reduce the tendency of the surfactant to aggregate [21].

A great work has been done on identifying the factors that determine CMC in aqueous solution, including the surfactant structure that plays a central role. In relation to the hydrophobic group, it is known that when the carbon–carbon double bond is present, CMC is higher than that of the corresponding saturated compound [21,22] which is contrary to the CMC values reported here. Another important factor that influences the CMC is the headgroup area of the surfactant; therefore, we calculated its value through the Gibbs adsorption equation. Briefly, classical theory indicates that the added surfactant adsorbs to the air-water interface and decreases the surface tension of water; at some point (i.e., CMC) micelles begin to assemble and the addition of the surfactant molecules will lead to the formation of micelles and no further decrease in surface tension occurs [23,24]. The theoretical analysis of soluble surfactant adsorption at the interface has been described by Gibbs adsorption Eqs. (1) and (2) [24],

$$\Gamma_{max} = -\frac{1}{2.303nRT}\left(\frac{\partial\gamma}{\partial \log[C10SA]}\right)_T \quad (1)$$

$$A_{min} = \frac{10^{18}}{N_A \Gamma_{max}} \quad (2)$$

where Γ_{max} represents maximum surface excess in mol/m^2, R = 8.314 J mol^{-1} K^{-1}, T = 298 K, γ represents the surface tension in mN/m, N_A is Avogadro's number (6.02×10^{23} mol^{-1}) and A_{min} is the surface area at the air water interface in nm^2. The parameter *n* represents the number of species at the interface whose concentration changes with surfactant concentration and in the presence of an electrolyte with a common counterion (i.e., sufficient salt to make electrostatic effects unimportant) [24–26], the value of *n* is taken to be unity [27].

It should be noted that, in the literature, there is some disagreement as to when and how the Gibbs equation may be safely used to interpret surface tension data; this discrepancy is ascribed to saturation at the interface. Menger et al. [28–30] explained that the decrease in surface tension as observed in Fig. 1 results from the type of cooperativity among amphiphilic ions or molecules; thus the interface is not saturated. On the other hand, Bermúdez-Salguero et al. [31] argued that surface saturation must precede micelle formation, suggesting that micelles form as a consequence of surface saturation. Mukherjee et al. [17] stated that Gibbs equation is thermodynamically correct, and the discrepancy goes either to the specificity of the system but not to the inadequacy of Gibbs equation which can extend up to CMC. Alternatives methods to the direct determination of surface excess at the air-water interface and thus the molecular area have been proposed, among them neutron reflectivity (NR) [32–34] or surface pressure-area (π - A) isotherms [33]. Accordingly, we used the value of the slope in the linear region (extended up to CMC) as shown in Fig. 1 and Eqs. (1)–(2) to obtain surface excess at the CMC (Γ_{max}) and A_{min} respectively (Table 1). The results obtained using the Gibbs methods were taken as approximate values, as is widely discussed in the literature.

In addition, we performed a study of monolayers at the air/water interface to gain information on the molecular area determined by Langmuir balance. Although it would be preferable to make comparisons forming a monolayer using C10SA, that was not possible because C10SA is too water-soluble for Langmuir balance studies. Indeed, we obtained stable monolayers at the air-water interphase using C16SA (Scheme 1 for n = 16) with a chain sufficiently long to form stable monolayers [35] on 0.15 M NaOH aqueous subphase.

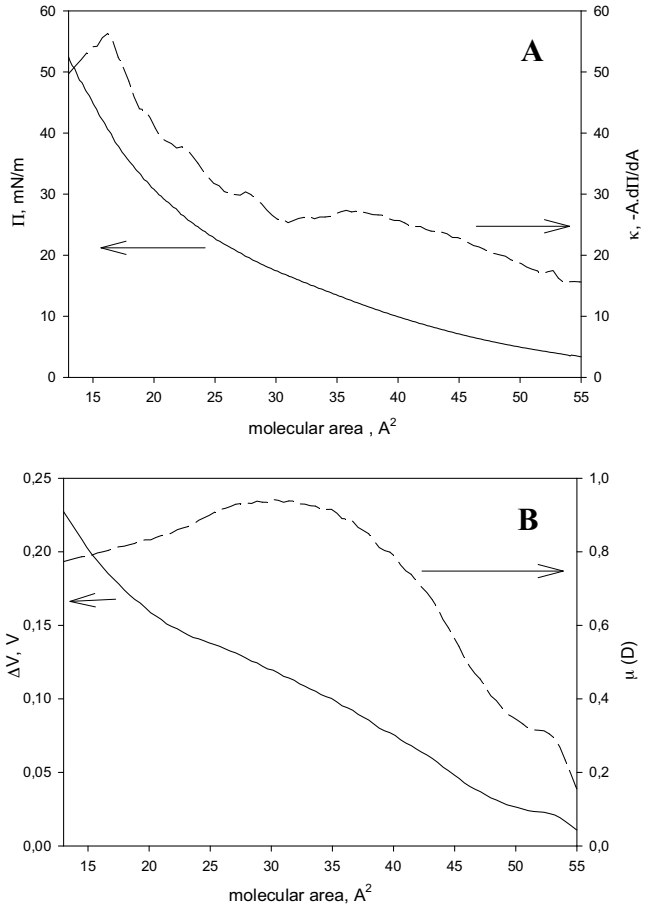

Fig. 2. (A) Variation of surface pressure (solid line) and surface compressional modulus (dashed line) with molecular area for C16SA and (B) the variation of surface potential (solid line) and perpendicular resultant dipole moment (dashed line) with molecular area. The aqueous sub-phase is 0.15 M NaOH.

The similarity between the molecular area values measured in Langmuir monolayers with those determined by surface tension, was also noted by others authors. For instance, Mukherjee et al. [17] reported that the minimum area per molecule for octadecyltrimethylammonium bromide, determined by surface tension measurement was similar to that obtained from Langmuir monolayer measurements. Besides, using the data reported by Nakahara et al. [36] regarding the surface adsorption of sodium dodecyl sulfate (SDS); we observed that from the extrapolation to the abscissa of the slope of the surface pressure-mean molecular area isotherm (π-A) up to a surface pressure of 50 mN/m, it is possible to obtain a molecular area of 0.5 nm^2 which matches the area reported in the literature for SDS [24,37]. Nevertheless, this last comparison was not mentioned in the article.

Fig. 2A shows the variation of surface pressure (solid line) and surface compressional modulus (dashed line) with molecular area. Fig. 2B depicts the variation of surface potential (solid line) and the perpendicular resultant dipole moment, (μ, dashed line) with molecular area. Fig. 2A-B reveals a large variety of packing states along the compression isotherm. The intermolecular organization adopted by C16SA implies a major reorganization of the hydrophobic and hydrophilic moieties of C16SA molecules in the films depending on the lateral surface pressure. Some of the features are described as follows:

During compression, at about 5 mN/m and molecular packing less than 50 Å^2, the film goes into a condensed liquid state and remains in a similar state, from a surface pressure of 5 mN/m to 18 mN/m approximately (about 50–30 Å^2). This is evidenced by the plateau values of the surface compressional modulus κ (with values between 17 and 27 mN/m) which correspond to films having a rather condensed liquid state. At 20 mN/m (28 Å^2) approximately, a change in the slope of μ -molecular area isotherm occurs in a very condensed film (solid condensate state) which is clearly noticeable by the further increase in the values of the surface compressional modulus κ.

The results demonstrated that resultant dipole moment reorientations and intermolecular organizations can be achieved by C16SA through the control of surface pressure at molecular packing ~35 Å^2 (at a surface pressure ~16 mN/m) and at the limiting mean molecular area of about 18 Å^2 (at the collapse pressure of 56 mN/m). The limiting molecular area corresponds to the cross-sectional area of alkyl chain [23,16], and indicates that the monolayers have collapsed after the closest molecular packing. The average molecular area at ~35 Å^2 is in agreement with the value found in literature for a unique carboxylate group (the molecular area for sodium dodecanote [24] and hexadecanoate [24] are 47 Å^2 and 31 Å^2 respectively) and also matches the molecular area determined by surface tension measurement (A_{min} = 35 Å^2, Table 1).

Using a molecular modeling program [38], it was possible to estimate a possible conformation adopted by C10SA and its derivative that contains a saturated aliphatic chain (Scheme 2). In the calculations a *trans* conformation was assumed for the two carboxylate groups since under basic experimental conditions that is the favored one [39].

Regarding molecular conformation, one of the carboxylate groups is in the proximity of the double bond, probably due to a van der Waals radius smaller than that of a methylene group [40,41], which reduces the available area per surfactant molecule at the surface. Therefore, the small CMC observed for C10SA may be attributed to the close molecular packing that is allowed by the conformation of the polar head. A similar behavior was observed in quaternary cationic surfactants where the planar pyridinium derivates packed more easily than tetrahedral trimethylammonium surfactants [21]. Indeed, a NMR NOESY spectrum of a solution of C10SA in D_2O at pD ~ 11 (Fig. S7, Supplementary information) showed NOE effects, between the protons $H_{d,d'}$ and $H_{b,b'}$ indicating a close proximity (less than 5 Å).

To have another experimental demonstration of the importance of the double bond in the solution behavior of C10SA it would be useful to have data for the saturated derivative, therefore we synthetized the compound but under the same experimental conditions, it was not possible to solubilize it even heating up to 80 °C. This result is another significant probe that the double bond plays a crucial role in the solubilization and packing of the C10SA molecules in the micellar assemblies.

3.2. Hydrodynamic radius, R_H

A DOSY (Diffusion Ordered SpectroscopY) spectrum was collected using a solution of [C10SA] = 5 mM (far above CMC) at pD~11. The DOSY spectrum (Fig. S8 in Supplementary information) is a 2-D experiment that shows proton chemical shifts in the horizontal axis and diffusion coefficients in the vertical axis. All the signals of C10SA appeared at a diffusion coefficient value of 0.55×10^{-10} m^2/s, and by using this value we calculated R_H = 0.4 nm (Table 1). Dynamic light scattering (DLS) lead to a similar R_H value, namely 0.9 nm (Table 1) calculated from the hydrodynamic diameter of C10SA (d_{app} = (1.8 ± 0.6) nm). The discrepancy in the value of R_H obtained by DOSY and DLS is expected considering the differences in the techniques used [42], and the values of R_H are comparable with that reported for micelles of ammonium decanoate (R_H = 1.6 nm) [43].

15

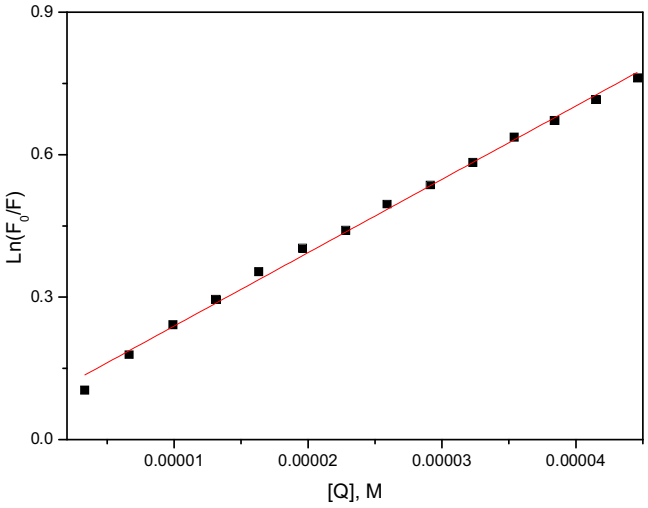

Fig. 3. Change in fluorescence intensity of a solution of [pyrene] = (2×10^{-6} M) and [C10SA] = 4.7×10^{-3} M as a function of cetylpyridinium chloride (Q), λ_{exc} = 335 nm, and λ_{em} = 392 nm.

3.3. Mean aggregation number

It is well known that the intensity ratio of a probe in the presence (F) and absence (F_0) of a quencher (Q) is related to the aggregation number (n_{agg}), the quencher concentration and the total concentration of a given surfactant ([Det]), as shown by Eq. (3) [44].

$$Ln\frac{F_0}{F} = \frac{[Q].n_{aag}}{[Det] - CMC} \quad (3)$$

In this study, we used pyrene and cetylpyridinium chloride (Q) as a donor and quencher of luminescence respectively [45]. The data obtained (Fig. 3) were fitted to Eq. (3); from the slope of the plot and using $CMC_{average}$ = 0.6 mM (mentioned above), n_{agg} = (55 ± 5) molecule/micelle was calculated. This value is in the order reported for ionic surfactants containing a single long alkyl chain [21], and comparable with the n_{agg} values reported for micelles of sodium [46] and ammonium [43] decanoate (38 and 54 molecules/micelle respectively). As mentioned before, it seems to us that the arrangements of carboxylate groups in the C10SA molecules (Scheme 2) result in a decrease in their mutual steric and electronic repulsion in the micelle, allowing a closer packing of the head groups.

3.4. Micellar structure and shape

To predict the shape of the aggregates, we did not attempt to calculate the molecular packing parameter [21,47] since we were not able to determine the length of the surfactant tail. Due to the disposition of carboxyl groups of C10SA (Scheme 2) the hydrophobic core is difficult to define. The micellar structure of C10SA was estimated from geometric constraints, assuming a spherical micelle with a radius R_H, made up of n_{agg} molecules, surface area of the micelle, A ($A = A_{min}.n_{agg}$), is given by Eq (4).

$$A_{min}.n_{agg} = 4.\pi.R_H^2 \quad (4)$$

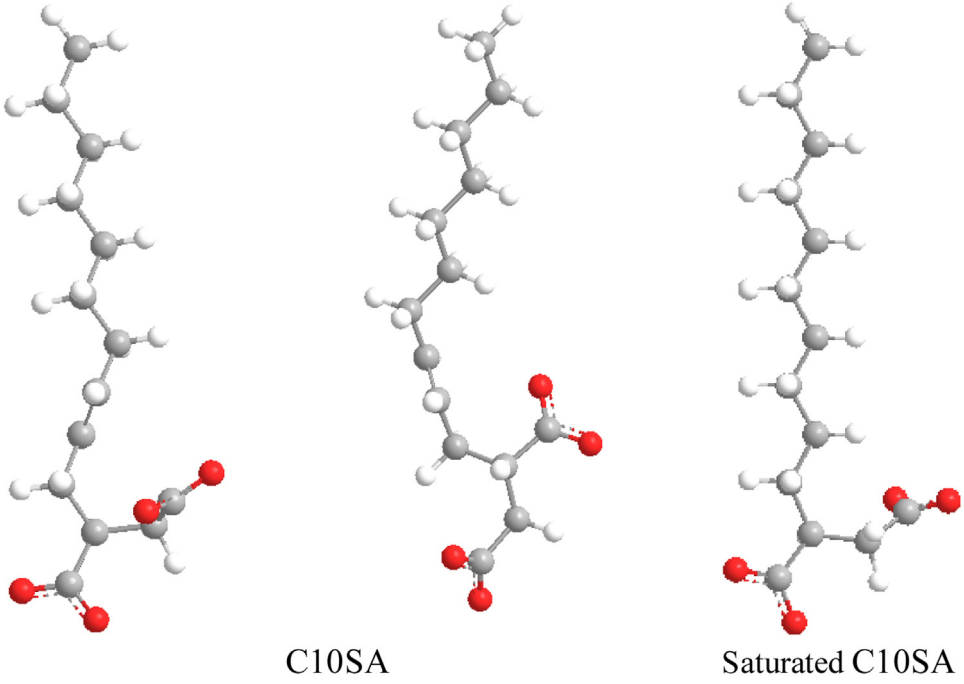

Scheme 2. Molecular model representations of C10SA and Saturated C10SA.

Using Eq. (4) and the values for A_{min} and n_{agg} (mentioned above), a value for R_H = 1.2 nm was calculated that is similar to the values determined by NMR and DLS (Table 1), thus geometrical arguments support the case for a spherical micelle.

4. Conclusions

The aggregation behavior of C10SA was extensively studied. Its CMC value is significantly lower than that of other surfactants of similar hydrocarbon chains but containing only one carboxylic group in the polar head. Among the factors to affect the CMC, we identified the role of the double bond and arrangement of carboxyl groups in the hydrophilic head. The arrangement of the carboxyl groups plays a crucial role because it favors a better packing of the headgroup of the surfactant resulting in a reduction of their mutual repulsion in the micelle. The presence of the double bond seems to be very important to define the conformation, maintaining one of the carboxylic moieties close to it. This conformation influences the solubilization/aggregation behavior and is responsible in part of the interesting characteristics found in this simple molecule, as is the high tendency to self-assembly forming micelles of spherical shape and small size.

The particular arrangement of the C10SA carboxyl groups was confirmed from the calculation of the molecular area of the headgroup in Langmuir monolayer at the air/water interphase formed by C16SA.

Acknowledgments

This work was supported by SECyT-UNC (Res. 1565/14), MINCyT-CBA (PID 2009–2011), CONICET (PIP 112-201101-00441), FONCYT (PICT 2008-0180), Argentina. O.F.S, M.A.F and R. H .R. hold research positions at CONICET. We gratefully acknowledge to Raquel V. Vico (INFIQC-UNC-CONICET), and Bruno Maggio (CIQUIBIC-UNC-CONICET) for technical support in Langmuir balance measurements.

Appendix A. Supplementary data

Supplementary data associated with this article can be found, in the online version, at http://dx.doi.org/10.1016/j.colsurfa.2016.07.098.

References

[1] L. Candy, C. Vaca-Garcia, E. Borredon, Synthesis and characterization of oleic succinic anhydrides: structure-property relations, J. Am. Oil Chem. Soc. 82 (2005) 271–277.
[2] O.F. Silva, M.A. Fernández, S.L. Pennie, R.R. Gil, R.H. de Rossi, Synthesis and characterization of an amphiphilic cyclodextrin, a micelle with two recognition sites, Langmuir 24 (2008) 3718–3726.
[3] M.A. Hubbe, Paper's resistance to wetting—a review of internal sizing chemicals and their effects, BioResources 2 (2006) 106–145.
[4] D. Yu, Z. Lin, Y. Li, Octadecenylsuccinic anhydride pickering emulsion stabilized by g-methacryloxy propyl trimethoxysilane grafted montmorillonite, Colloids Surf. A: Physicochem. Eng. Aspects 422 (2013) 100–109.
[5] H. Wang, W. Liu, X. Zhou, H. Li, K. Qian, Stabilization of ASA-in-water emulsions by laponite modified with alanine, Colloids Surf. A: Physicochem. Eng. Aspects 436 (2013) 294–301.
[6] P. Ding, W. Liu, Z. Zhao, Roles of short amine in preparation and sizing performance of partly hydrolyzed ASA emulsion stabilized by laponite particles, Colloids Surf. A: Physicochem. Eng. Aspects 384 (2011) 150–156.
[7] T. Imae, B. Trend, Video-enhanced differential interference contrast microscope observation of pH-dependent vesicle formation by single chain surfactants, Langmuir 7 (1991) 643–646.
[8] K. Nakazawa, T. Imae, T. Iwamoto, Microscopic observation of vesicles formed by alkenylsuccinic acids, Langmuir 8 (1992) 1878–1880.
[9] C.J. González, R.H. de Rossi, Synthesis and complexation properties of an amphiphilic cyclodextrin, Arkivoc (2001) 87–99.
[10] J. Lindfors, J. Salmi, J. Laine, P. Stenius, Akd and asa model surfaces: preparation and characterization, BioResources 2 (2007) 652–670.
[11] G. Hemakanthi, A. Dhathathreyan, B. Nair, T. Ramasami, D. Mo, Control of Size of PbI_2 nanocrystals using Langmuir—Blodgett films of *n* -octadecyl Succinic acid, Colloids Surf. A: Physicochem. Eng. Aspects 181 (2001) 115–121.
[12] S. Hacke, D. Möbius, Influence of active sites distribution on $CaCO_3$ formation under model biofilms at the air/water interface, Colloid. Polym. Sci. 282 (2004) 1242–1246.
[13] R.A. Al-Horani, U.R. Desai, Electronically rich N -substituted tetrahydroisoquinoline 3-carboxylic acid esters: concise synthesis and conformational studies, Tetrahedron 68 (2012) 2027–2040.
[14] N.G. Akhmedov, E.M. Myshakin, C.D. Hall, Dynamic NMR and ab initio studies of exchange between rotamers of derivatives of octahydrofuro[3,4-F]isoquinoline-7(1H)-carboxylate and

tetrahydro-2,5,6(1H)-isoquinolinetricarboxylate, Magn. Reson. Chem. 42 (2004) 39–48.
[15] L.-H. Zhuang, K.-H. Yu, G.-W. Wang, C. Yao, Synthesis and properties of novel ester-containing gemini imidazolium surfactants, J. Colloid Interface Sci. 408 (2013) 94–100.
[16] R.V. Vico, O.F. Silva, R.H. de Rossi, B. Maggio, Molecular organization structural orientation, and surface topography of monoacylated beta-cyclodextrins in monolayers at the air-aqueous interface, Langmuir 24 (2008) 7867–7874.
[17] I. Mukherjee, S.P. Moulik, A.K. Rakshit, Tensiometric determination of gibbs surface excess and micelle point: a critical revisit, J. Colloid Interface Sci. 394 (2013) 329–336.
[18] A. Bhadani, S. Singh, Synthesis and properties of thioether spacer containing gemini imidazolium surfactants, Langmuir 27 (2011) 14033–14044.
[19] T. Namani, P. Walde, From decanoate micelles to decanoic acid/dodecylbenzenesulfonate vesicles, Langmuir 21 (2005) 6210–6219.
[20] R. Bordes, K. Holmberg, Physical chemical characteristics of dicarboxylic amino acid-based surfactants, Colloids Surf. A: Physicochem. Eng. Aspects 391 (2011) 32–41.
[21] M.J. Rosen, Surfactants and Interfacial Phenomena, Ed. Third, Wiley-Interscience, New York, 2004, pp. 105–177.
[22] J.M. Kuiper, R.T. Buwalda, R. Hulst, J.B.F.N. Engberts, Novel pyridinium surfactants with unsaturated alkyl chains: aggregation behavior and interactions with methyl orange in aqueous solution, Langmuir 17 (2001) 5216–5224.
[23] F.M. Menger, L. Shi, Electrostatic binding among equilibrating 2-D and 3-D self-assemblies, J. Am. Chem. Soc. 131 (2009) 6672–6673.
[24] M.J. Rosen, Surfactants and Interfacial Phenomena, Ed. Third, Wiley-Interscience, New York, 2004, pp. 34–104.
[25] K. Tsubone, Y. Arakawa, M.J. Rosen, Structural effects on surface and micellar properties of alkanediyl-alpha, omega-bis(sodium N-acyl-beta-alaninate) gemini surfactants, J. Colloid Interface Sci. 262 (2003) 516–524.
[26] J. Aslam, U.S. Siddiqui, I.A. Bhat, Kabir-ud-Din, Molecular interactions of cationic gemini surfactants (m-S-m) with an environmental friendly nonionic sugar-based surfactant (β-C12G): interfacial, micellar and aggregation behavior, J. Ind. Eng. Chem. 20 (2014) 3841–3850.
[27] In our experimental conditions the ionic strength was 0.2 M (swamping amount of electrolyte) therefore the value of *n* is taken to be unitary (see References 25–26).
[28] F.M. Menger, S.A.A. Rizvi, Relationship between surface tension and surface coverage, Langmuir 27 (2011) 13975–13977.
[29] F.M. Menger, L. Shi, S.A.A. Rizvi, Additional support for a revised gibbs analysis, Langmuir 26 (2010) 1588–1589.
[30] F.M. Menger, L. Shi, S.A.A. Rizvi, Re-evaluating the gibbs analysis of surface tension at the air/water interface, J. Am. Chem. Soc. 131 (2009) 10380–10381.
[31] C. Bermúdez-Salguero, J. Gracia-Fadrique, Analysis of gibbs adsorption equation and thermodynamic relation between gibbs standard energies of adsorption and micellization through a surface equation of state, J. Colloid Interface Sci. 355 (2011) 518–519.
[32] H. Xu, P.X. Li, K. Ma, R.K. Thomas, J. Penfold, J.R. Lu, Limitations in the application of the gibbs equation to anionic surfactants at the air/water surface: sodium dodecylsulfate and sodium dodecylmonooxyethylenesulfate above and below the CMC, Langmuir 29 (2013) 9335–9351.
[33] P.X. Li, Z.X. Li, H.-H. Shen, R.K. Thomas, J. Penfold, J.R. Lu, The application of the gibbs equation to the adsorption of nonionic surfactants and polymers at the air-water interface: comparison with surface excesses determined directly using neutron reflectivity, Langmuir 29 (2013) 9324–9334.
[34] J. Eastoe, S. Nave, A. Downer, A. Paul, A. Rankin, J. Penfold, Adsorption of ionic surfactants at the air—solution interface, Langmuir 16 (2000) 4511–4518.
[35] Due the presence of two carboxylate groups in the headgroup, about 90% of C16SA molecules initially spread at the interface are quickly lost into the aqueous sub-phase ([NaOH] = 0.145 M); however, the rest of the material forms stable films at the interface with no film loss, undergoing reproducible surface pressure dependent reorganization under compression and decompression cycles. All the surface pressure-molecular area isotherms reported in this work correspond to those calculated with the measured amount of C16SA present at the interface (the latter was determined by ^{1}HNMR using benzoic acid as the internal standard and taking the difference between the total amount used and the quantity directly measured in the sub-phase).
[36] H. Nakahara, O. Shibata, Y. Moroi, Examination of surface adsorption of cetyltrimethylammonium bromide and sodium dodecyl sulfate, J. Phys. Chem. B 115 (2011) 9077–9086.
[37] M.A. James-Smith, K. Alford, D.O. Shah, A novel method to quantify the amount of surfactant at the oil/water interface and to determine total interfacial area of emulsions, J. Colloid Interface Sci. 310 (2007) 590–598.
[38] The structures were obtained using the modeling programs ChemBio 3D ultra with the *abinitio* calculation program GAMESS and Gaussian 03W.
[39] F. Wang, Y.-H. Zhang, L.-J. Zhao, H. Zhang, H. Cheng, J.-J. Shou, Micro-Raman study on the conformation behavior of succinate in supersaturated sodium succinate aerosols, Phys Chem. Chem. Phys. 10 (2008) 4154–4158.
[40] B. Rijksen, S.P. Pujari, L. Scheres, C.J.M. Van Rijn, J.E. Baio, T. Weidner, H. Zuilhof, Hexadecadienyl monolayers on hydrogen-terminated Si(111): faster monolayer formation and improved surface coverage using the enyne moiety, Langmuir 28 (2012) 6577–6588.
[41] L. Scheres, B. Rijksen, M. Giesbers, H. Zuilhof, Molecular modeling of alkyl and alkenyl monolayers on hydrogen-terminated Si(111), Langmuir 27 (2011) 972–980.
[42] D.P. Hinton, C.S. Johnson, Diffusion ordered 2D NMR spectroscopy of phospholipid vesicles: determination of vesicle size distributions, J. Phys. Chem. 97 (1993) 9064–9072.
[43] R.M. Clapperton, R.H. Ottewill, A.R. Rennie, B.T. Ingram, Comparison of the size and shape of ammonium decanoate and ammonium dodecanoate micelles, Colloid. Polym. Sci. 277 (1999) 15–24.
[44] N.J. Turro, A. Yekta, Luminescent probes for detergent solutions a simple procedure for determination of the mean aggregation number of micelles, J. Am. Chem. Soc. 100 (1978) 5951–5952.
[45] M.F. Torres, R.H. de Rossi, M.A. Fernández, Aggregation behavior of perfluorononanoic acid/sodium dodecyl sulfate mixtures, J. Surfactants Deterg. 16 (2013) 903–912.
[46] H. Huang, R.E. Verrall, Thermodynamic and aggregation behavior of mixed micellar systems of sodium decanoate and ethoxylated alcohols in water at 25 °C, J. Solut. Chem. 26 (1997) 135–162.
[47] R. Nagarajan, Molecular packing parameter and surfactant self-assembly: the neglected role of the surfactant tail, Langmuir 18 (2002) 31–38.